Abstract

The potential of double-skin façade systems as distributed mass dampers to reduce vibrations in tall buildings under seismic excitations is investigated in this paper. The design problem consists of determining flexural stiffness of the outer skin, as well as the stiffness of its links to the primary structure and its damping. These structural parameters are estimated through two alternative optimisation procedures, aiming at minimising the standard deviation of the displacements of the first storey of the primary structure. Numerical results are presented for a set of recorded accelerograms to take into account the effects of non-stationary excitations. A direct approach for the design of the stiffness link is also presented, based on observations deriving from the outcome of the optimisation problem.

Keywords: Earthquake engineering, double-skin façades, non-classically damped structures, structural optimisation, tuned-mass dampers, vibration absorbers.

1 Introduction

A double-skin façade (DSF) consists of a multi-layered building envelope with a ventilated cavity between outer and inner glazing skins. This system has many advantages, as it allows combining the efficiency of an improved control of the indoor environment (in terms of air flow, heat flow and noise) with the aesthetically pleasant transparency of all-glass façades. From the structural engineering point of view, the outer skin of the building envelope can be considered as a secondary attachment to the primary load-bearing structure, whose safety has to be checked for all the design scenarios, including wind forces and (for earthquake-prone sites) seismic forces. This gives rise to a coupled dynamic problem for the combined primary-secondary system, and different analysis methods can be used to calculate

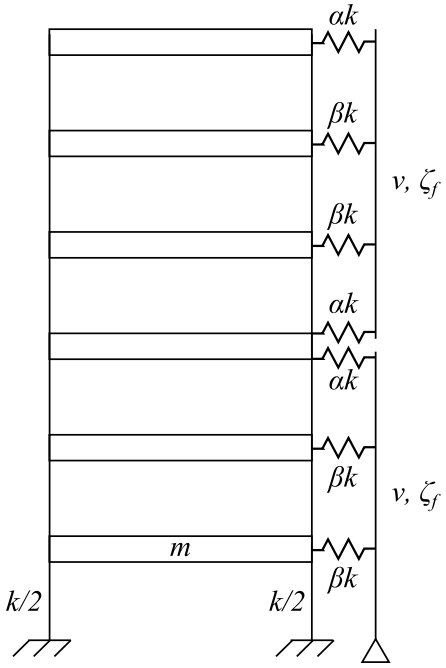

Figure 1: Shear-type primary structure with double-skin façade.

the response of the main structure and the attachment. In a typical design situation, the DSF anchorage has to be stiff enough to avoid significant dynamic effects on the outer skin, therefore minimising the risk of damage accumulation due to the wind action or expensive (and dangerous) failures in case of intense seismic events. Alternatively, as per any secondary attachment, the vibration of the outer skin can be exploited to reduce the dynamic response of the building, provided that the secondary subsystem is properly tuned to the primary one. This innovative use of DSFs has been recently proposed by Moon [8,9] as a way to control wind-induced vibrations in tall buildings, while Abtahi et al. [1] and Fu [3] have successively studied the effects of a flexible outer skin on the seismic response of the primary structure.

In this paper, a preliminary study on DSFs as distributed vibration absorbers for multi-storey buildings is reported. The response of the coupled system composed by the primary structure and the DSF is obtained as a function of four parameters representative of the damping and flexural stiffness of the DSF and of the stiffness of its links with the primary structure. The design problem is approached, in first instance, as an optimisation problem, minimising the standard deviation of the response of the primary structure for a set of seismic accelerograms. Results are obtained by both Genetic Algorithms (GAs) and Particle Swarm Optimisation (PSO). Then, in light of the results obtained by such procedure, a more direct approach is investigated for the specific design of the links between the DSF and the primary structure.

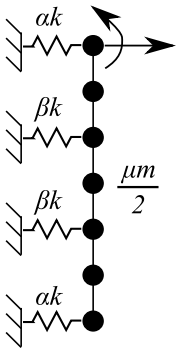

Figure 2: Lumped mass system for the double-skin substructures.

2 Structural model

In this paper, a case study has been used to investigate and quantify the effectiveness of double-skin façades (DSFs) for reducing the vibration in multi-storey buildings subjected to seismic ground motions. In order to provide a realistic assessment of the seismic performance of this solution, a set of 20 earthquake records, listed in Table 1, has been considered as external excitations on the system.

The mathematical model adopted for the coupled structural system is sketched within Figure 1. The primary structure is a six-storey, classically damped, shear-type moment-resisting frame. It has been assumed that the storeys have all equal mass m and stiffness k, while ζ is the viscous damping ratio.

The DSF has been divided in two substructures: a first panel, hinged to the ground and connected to the three bottom storeys of the frame; and a second panel, solely connected to the upper three storeys (see Figure 1). Other configurations might be possible, e.g. a continuous DSF throughout the whole height of the primary frame, or one panel for each storey, which however have not been considered in this paper. The flexural stiffness of each panel has been assumed to be proportional to the stiffness k of the primary structure according to a coefficient ν. The links between the primary structure and each panel of the DSF have been idealised as elastic springs with stiffness proportional to k, as well, according to two additional coefficients of proportionality, α and β, for the external and internal springs, respectively.

Each panel has been modelled as a lumped mass system, as shown within Figure 2. Each mass takes into account for half of the inter-storey mass of the panel, so that each secondary lumped mass is $\mu m/2$, where μ is the mass ratio between the total mass of the primary structure and the total mass of the DSF. Horizontal displacements and rotations of each mass have been considered as DoFs (degrees of freedom) of the panel. Overall, the combined system has $6+12+12=30$ DoFs.

If the coupled system (primary structure and DSF) is undamped, its motion is governed by the following system of equations:

$$\mathbf{M}\cdot\ddot{\mathbf{x}}(t)+\mathbf{K}\cdot\mathbf{x}(t)=-\mathbf{M}\cdot\boldsymbol{\tau}\ddot{x}_g(t)\,, \tag{1}$$

Table 1: Earthquake records considered for the numerical applications

Accelerogram	Epicentre	Date	Peak acceleration (g)	Duration
1	PARKFIELD, CALIFORNIA	27/06/1966	0.434	44.04
2	PACOIMA DAM, CALIFORNIA	09/02/1971	1.075	41.74
3	HELENA, MONTANA	31/10/1935	0.147	50.96
4	WRIGHTWOOD, CALIFORNIA	12/09/1970	0.198	16.72
5	LAKE HUGHES, CALIFORNIA	09/02/1971	0.146	37.02
6	IVERSON, CANADA	23/12/1985	1.102	20.34
7	YONEYAMA BRIDGE, JAPAN	26/02/1971	0.151	17.06
8	EL CENTRO, CALIFORNIA	18/05/1940	0.348	53.74
9	T. LINCOLN SCHOOL TUNNEL, CALIFORNIA	21/07/1952	0.179	54.40
10	MONTE NEGRO, YUGOSLAVIA	19/04/1979	0.171	40.40
11	LA VILLITA, GUERRERO ARRAY, MEXICO	19/09/1985	0.123	64.02
12	EL CENTRO, CALIFORNIA	30/12/1934	0.160	44.04
13	STURNO, ITALY	11/11/1980	0.358	39.34
14	DUZCE, TURKEY	12/11/1999	0.535	25.89
15	TAKATORI, JAPAN	16/01/1995	0.611	40.96
16	TABAS, IRAN	16/09/1978	0.836	32.84
17	ERZIKAN, TURKEY	13/03/1992	0.515	21.31
18	KALAMATA, GREECE	13/09/1986	0.248	12.19
19	LOMA PRIETA, CALIFORNIA	18/10/1989	0.966	25.00
20	TOLMEZZO, ITALY	06/05/1980	0.351	36.35

where $\mathbf{M}$ and $\mathbf{K}$ are mass and stiffness matrices of the coupled system, respectively; $\mathbf{x}(t)$ is the vector collecting displacements and rotations of the system masses; $\boldsymbol{\tau}$ is the location vector; and $\ddot{x}_g(t)$ is the ground acceleration.

The mass matrix $\mathbf{M}$ and the stiffness matrix $\mathbf{K}$ are defined as the following block matrices:

$$\mathbf{M}=\begin{bmatrix} \mathbf{M}_0 & \mathbf{O} & \mathbf{O} \\ \mathbf{O} & \mathbf{M}_1 & \mathbf{O} \\ \mathbf{O} & \mathbf{O} & \mathbf{M}_2 \end{bmatrix};\quad \mathbf{K}=\begin{bmatrix} \mathbf{K}_0 & \mathbf{K}_{01}^T & \mathbf{K}_{02}^T \\ \mathbf{K}_{01} & \mathbf{K}_1 & \mathbf{O} \\ \mathbf{K}_{02} & \mathbf{O} & \mathbf{K}_2 \end{bmatrix}, \tag{2}$$

where $\mathbf{M}_0$, $\mathbf{M}_1$ and $\mathbf{M}_2$ are the mass matrices of the primary structure and of the two panels, respectively; $\mathbf{K}_0$, $\mathbf{K}_1$ and $\mathbf{K}_2$ are the corresponding stiffness matrices; $\mathbf{K}_{01}$ and $\mathbf{K}_{02}$ contain the stiffness terms αk and βk of the elastic springs coupling the primary structure with the DSF; and $\mathbf{O}$ is a zero matrix of appropriate dimensions.

Since no inertia force is associated to the rotations of the lumped masses, the size of the Equation system (1) can be reduced by using the static condensation

technique [2]. To do this, the equations of motion are conveniently rewritten in the form:

$$\begin{cases} \mathbf{M}_{tt} \cdot \ddot{\mathbf{x}}_t(t) + \mathbf{K}_{tt} \cdot \mathbf{x}_t(t) + \mathbf{K}_{tr} \cdot \mathbf{x}_r(t) = -\mathbf{M}_{tt} \cdot \boldsymbol{\tau}_t \ddot{x}_g \ ; \\ \mathbf{K}_{rt} \cdot \mathbf{x}_t(t) + \mathbf{K}_{rr} \cdot \mathbf{x}_r(t) = \mathbf{0} \ , \end{cases} \tag{3a,b}$$

where $\mathbf{x}_t(t)$ contains all the lateral displacement components of the vector $\mathbf{x}(t)$, while $\mathbf{x}_r(t)$ collects all the rotations. By solving the algebraic Equation system (3b), and substituting the result in the system of differential Equations (3a), a new set of equations is obtained:

$$\mathbf{M}_{tt} \cdot \ddot{\mathbf{x}}_t(t) + \tilde{\mathbf{K}}_{tt} \cdot \mathbf{x}_t(t) = -\mathbf{M}_{tt} \cdot \boldsymbol{\tau}_t \ddot{x}_g \ , \tag{4}$$

where the condensed stiffness matrix $\tilde{\mathbf{K}}_{tt}$ is defined as:

$$\tilde{\mathbf{K}}_{tt} = \mathbf{K}_{tt} - \mathbf{K}_{tr} \cdot \mathbf{K}_{rr}^{-1} \cdot \mathbf{K}_{rt} \ . \tag{5}$$

In the following, the more general damped case has been analysed. Specifically, the damping matrix of the condensed system has been obtained by using the classic theory of modal analysis, assuming that the primary structure and the two double-skin substructures are, individually, classically damped. It is worth to stress that, however, the whole coupled system is not classically damped [5,10,11,6].

3 Design strategies

3.1 Optimisation of the DSF parameters

The design process of the DSF system proposed in the previous section requires determining the three coefficients $\{\nu, \alpha, \beta\}$ governing the stiffness of the DSF system, and its viscous damping coefficient ζ_f. A reasonable way to estimate the optimum values for the four parameters is to minimise a significant function (such as the standard deviation or the maximum peak) of the structural response.

In this paper, for each earthquake record of Table 1, the standard deviation of the displacements of the first storey of the primary structure, $\sigma\left(x_1^C\right)$, has been minimised. The optimisation problem has been formulated as follows:

$$
\begin{aligned}
&\text{Given:} && m, k, \zeta, \ddot{x}_g, \text{geometry};\\
&\text{Find:} && \zeta_f, \nu, \alpha, \beta;\\
&\text{To minimise:} && \sigma\left(x_1^C\right);\\
&\text{Such that:} && \begin{cases} \zeta_{\min} \le \zeta_f \le \zeta_{\max}; \\ \nu_{\min} \le \nu \le \nu_{\max}; \\ \alpha_{\min} \le \alpha \le \alpha_{\max}; \\ \beta_{\min} \le \beta \le \beta_{\max}. \end{cases}
\end{aligned} \tag{6}
$$

Without lack of generality, the numerical applications here presented have been performed considering unitary masses for the 6 storeys of the primary frame, whose fundamental period of vibration and viscous damping ratio have been chosen as $T_1 = 0.583\,\text{s}$ and $\zeta = 0.02$; furthermore, $\mu = 0.1$ is the mass ratio between the building and the DSF. The ranges of variation of the four DSF parameters have been selected as follows:

$$
\begin{aligned}
&\zeta_f \in \left[\ 10^{-4};\ \ 2\times10^{-1}\ \right];\\
&\nu \in \left[\ 10^{-6};\ \ 5\times10^{-1}\ \right];\\
&\left(\alpha,\beta\right) \in \left[\ 10^{-6};\ \ 10^{-1}\ \right].
\end{aligned} \tag{7}
$$

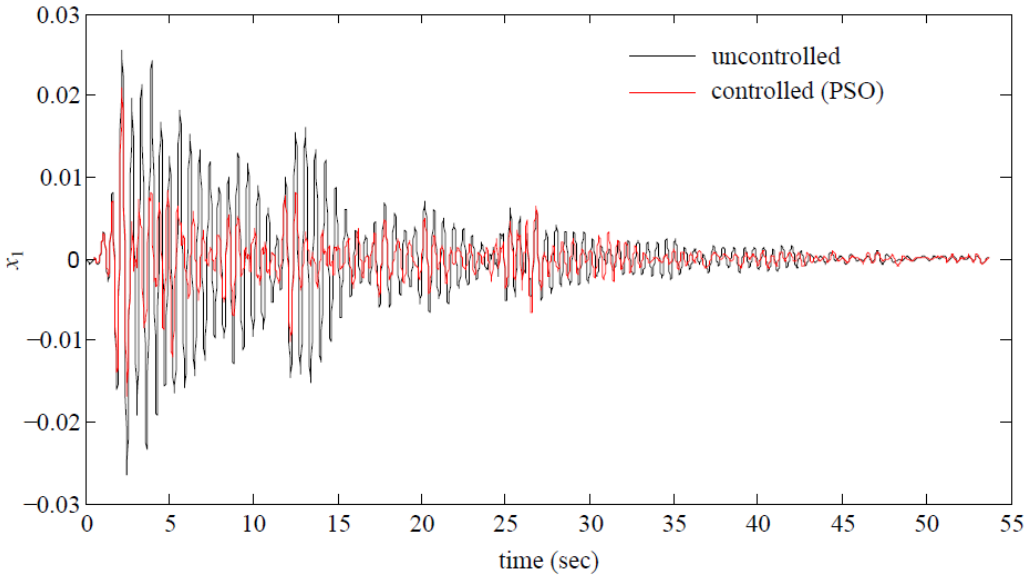

Figure 3: First storey displacements for El Centro 1940 earthquake: uncontrolled vs controlled system.

Both Genetic Algorithms (GA) and Particle Swarm Optimization (PSO) techniques have been considered to solve the optimisation problem. The GA is an iterative procedure in which a randomly generated initial population (sample of possible solutions) "evolves" towards the optimal one by using cross-over of single "individuals" (creating new individuals from two "parents"), mutation (random change of a parameter in an individual) and other evolutionary-like processes [4]. In the PSO, instead, tentative solutions behave as moving particles, whose trajectories and velocities, at each iteration, are influenced by local and global best solutions in the search space [7].

Figure 3 shows the time histories of the displacements computed for the first storey of the uncontrolled and controlled primary structure when subjected to the El Centro 1940 earthquake (accelerogram 8). The optimal parameters obtained by the PSO have been considered for the DSF panels, and the visual comparison confirms their excellent performance as vibration absorbers.

The results obtained by running the two numerical optimisation procedures are offered in Table 2. In particular, the estimated optimal parameters are shown together with the performance index p, defined as the percentage reduction in the displacement standard deviation of the first storey of the primary structure, which is proportional to the maximum base shear in the primary frame:

$$p = 1 - r = 1 - \frac{\sigma\left(x_1^C\right)}{\sigma\left(x_1^U\right)}. \tag{8}$$

In Equation (8), $\sigma\left(x_1^U\right)$ and $\sigma\left(x_1^C\right)$ represent the standard deviations of the uncontrolled and controlled systems, respectively, and r is their ratio. At first glance, all optimal parameters depend on the selected excitations. Also, GA and PSO return different solutions for each case; however, only very small variations of the performance parameter are observed for the same accelerogram. The PSO performs better than the GA, that is, for a selected earthquake record, the optimal solution obtained by PSO returns a larger performance index p with respect to the GA. However, in two specific cases (accelerograms 2 and 19) the PSO did not manage to locate any combination of the DSF parameters associated with a positive value of the performance index p; for this reason, these solutions have not been reported. Interestingly, in all cases but one the PSO return, as optimal value, the lower boundary selected for either α or β. The physical meaning of such behaviour is that only 2 of the four elastic links proposed in the initial model are actually needed to obtain the best performance for the DSF. It is worth to stress that, based on the PSO results, the DSF manages to reduce the standard deviation of the measured response to about half of its initial value, showing considerable potential for non-stationary applications.

Table 2: Optimal parameters and performance index by GA and PSO.

Accelerogram	Genetic Algorithm					Particle Swarm Optimization				
	ζ_f	ν	α	β	$p(\%)$	ζ_f	ν	α	β	$p(\%)$
1	0.1399	0.3056	0.0022	0.0046	54.52	0.1404	0.1413	$\alpha_{\min}$	0.0075	55.21
2	0.0472	0.2938	0.0058	0.0003	45.34	-	-	-	-	-
3	0.1961	0.4366	0.0004	0.0068	45.32	0.1586	0.1215	$\alpha_{\min}$	0.0082	46.03
4	0.1328	0.3273	0.0018	0.0068	55.31	0.1155	0.0970	$\alpha_{\min}$	0.0098	56.14
5	0.0546	0.0400	0.0481	0.0009	64.57	0.0460	0.0530	0.0389	$\beta_{\min}$	65.21
6	0.0639	0.0465	0.0408	0.0001	45.15	0.0629	0.0481	0.0364	$\beta_{\min}$	45.24
7	0.1206	0.1119	0.0044	0.0039	58.49	0.1243	0.1084	$\alpha_{\min}$	0.0093	59.67
8	0.1279	0.1226	0.0019	0.0047	47.91	0.0496	0.5000	0.0068	$\beta_{\min}$	50.27
9	0.0733	0.1448	0.0056	0.0018	40.66	0.1263	0.1256	$\alpha_{\min}$	0.0075	41.94
10	0.0994	0.1677	0.0037	0.0046	53.63	0.1001	0.1426	$\alpha_{\min}$	0.0095	54.91
11	0.1192	0.0532	0.0006	0.0084	57.81	0.0975	0.0852	$\alpha_{\min}$	0.0096	58.77
12	0.1038	0.0302	0.0029	0.0043	61.00	0.0832	0.1663	$\alpha_{\min}$	0.0079	62.48
13	0.1692	0.0921	0.0002	0.0086	39.47	0.1158	0.0748	0.0260	$\beta_{\min}$	39.43
14	0.1961	0.0035	0.0020	0.0035	30.34	0.1302	0.1121	$\alpha_{\min}$	0.0062	32.49
15	0.1433	0.0644	0.0039	0.0039	46.29	0.1384	0.0813	$\alpha_{\min}$	0.0089	46.67
16	0.1152	0.0626	0.0364	0.0000	45.24	0.1924	0.1014	$\alpha_{\min}$	0.0062	45.31
17	0.1095	0.4837	0.0050	0.0009	45.36	0.0660	0.5000	0.0059	0.0001	45.95
18	0.0754	0.0451	0.0034	0.0039	65.12	0.0810	0.1683	$\alpha_{\min}$	0.0078	65.70
19	0.0698	0.0002	0.9995	0.9976	23.69	-	-	-	-	-
20	0.1976	0.4807	0.0067	0.0025	39.55	0.1500	0.0811	$\alpha_{\min}$	0.0120	40.57

3.2 Link design

The realisation of the DSF panels for assigned flexural stiffness and damping (i.e. for given ν and ζ_f) may be not feasible in practical applications, in which case the values of ν and ζ_f would be assigned a priori. In light of the results obtained by the PSO, the authors have then investigated the relationship between the parameters α and β, representing the normalised stiffness of the elastic links between primary structure and DSF, in the attempt to achieve a direct design approach that avoids the burden of the numerical optimisation. In particular, in the following $\zeta_f = 0.11$ and $\nu = 0.15$ have been selected, as these are the values obtained as the average of the 18 meaningful PSO optimisations. Interesting, very similar average values have been obtained with the 20 GA optimisations.

For assigned ζ_f and ν, the performance index of Equation (8) depends only on the stiffness of the links. The ratio of the standard deviation of controlled and

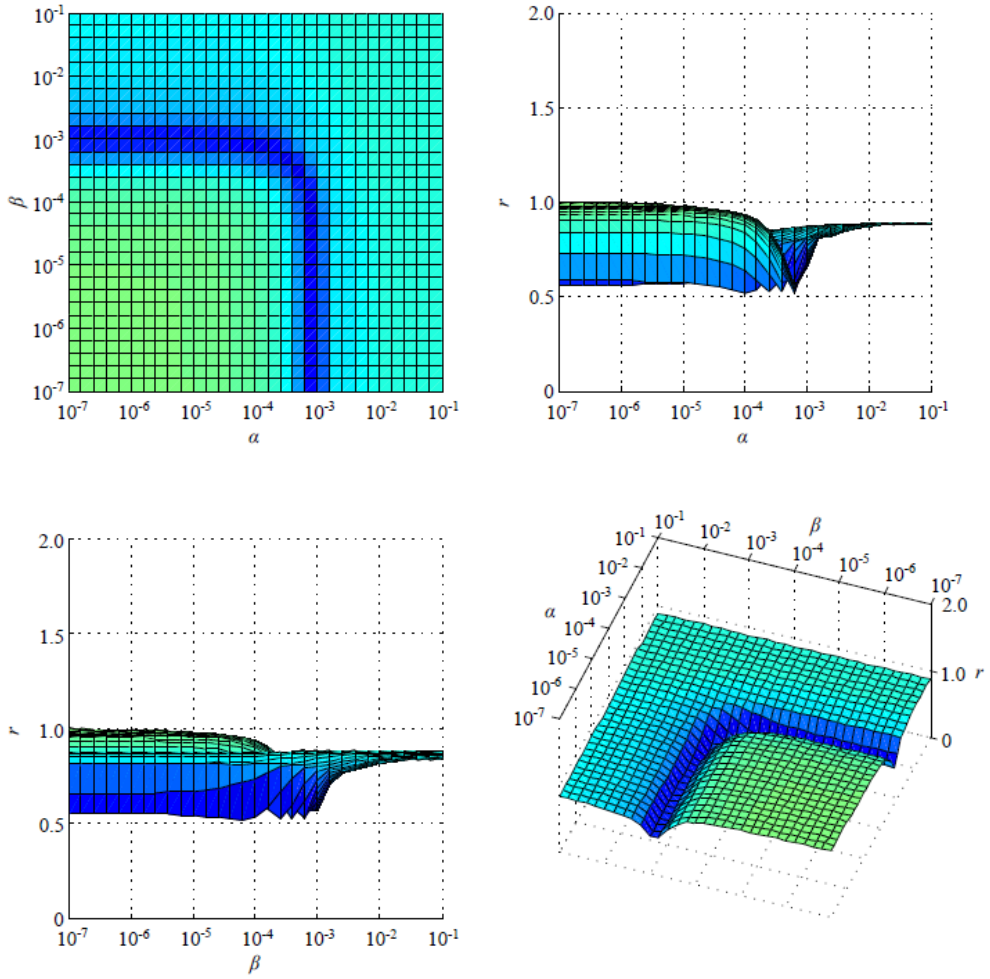

Figure 4: Function $r(\alpha,\beta)$, earthquake in El Centro 1940, California.

uncontrolled system, $r(\alpha,\beta)$, can in this case be represented as a response surface in the three-dimensional space. This is shown within Figures 4 and 5, where the colour map (top-left), a three-dimensional view (bottom-right) and two side views (top-right and bottom-left) are offered for two different base excitations (namely, El Centro 1940 and Loma Prieta 1989).

A common pattern is easily recognised in these response surfaces: i.e. a clear valley can be noticed, corresponding to the dark-blue narrow areas in the colour maps. In both cases, these optimal areas have two almost orthogonal branches that run parallel to the α-axis and β-axis and are then connected by a rounded bend with a relatively small radius of curvature (in the logarithmic scale used for both α and β). This observation suggests the possibility of identifying an analytical relationship between α and β, which could be used for designing the links. It has been also noticed that, in most cases, the actual optimal solution is obtained by either selecting $\alpha=\alpha_{\min}$ or $\beta=\beta_{\min}$ (i.e. one of the extreme locations of the dark-blue valleys). Interestingly, completely different dynamics of the DSF panels are associated with these two cases. Specifically, for $\alpha=\alpha_{\min}$, relatively large

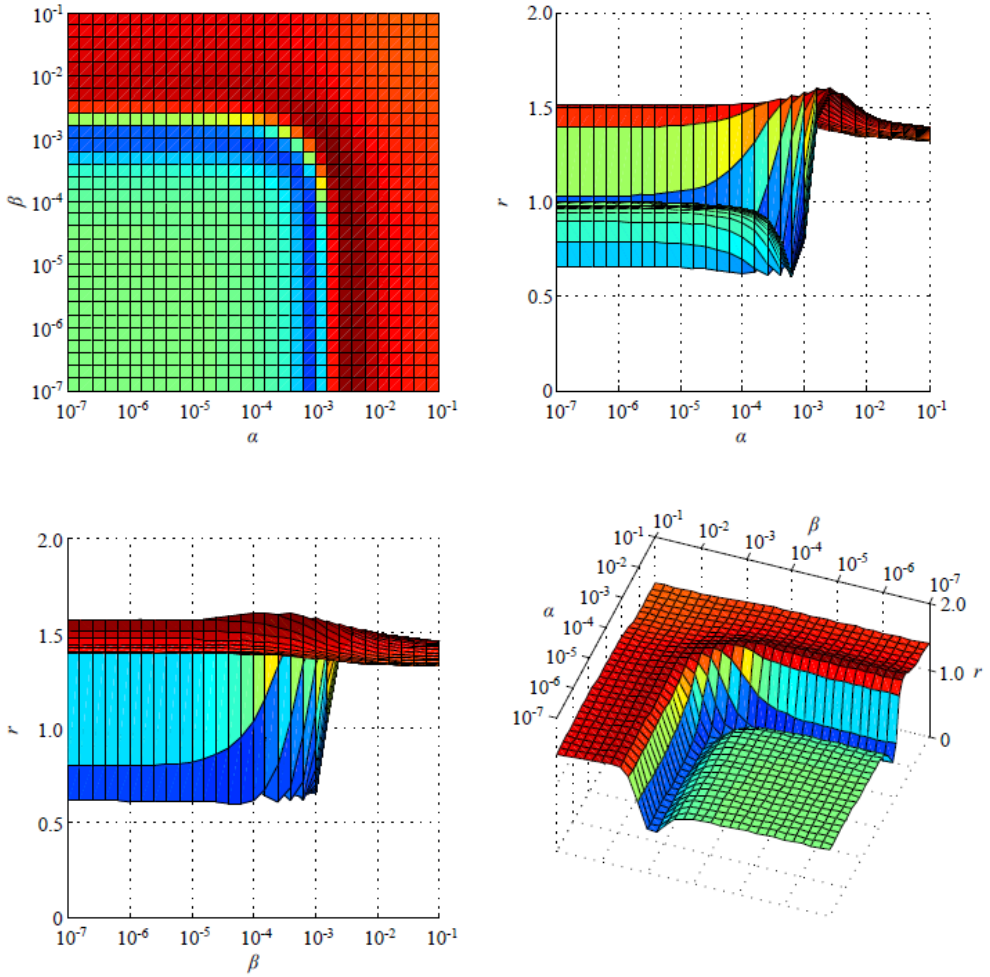

Figure 5: Function $r(\alpha,\beta)$, earthquake in Loma Prieta 1989, California.

deflections happens at the top and bottom ends of the DSF panels; while for $\beta = \beta_{\min}$, the maximum movements in the DSF panels tend to happen at their mid span position.

In Figure 6, the seismic responses for two different configurations of the controlled primary frame are compared for the case of the El Centro 1940 earthquake. The two configurations are obtained using: *i*) the optimal parameters returned by the PSO (red line, with DSF parameters offered within Table 2); and *ii*) designing the link stiffness following the procedure described in this Section (blue line). Only minor differences can be seen between the two time histories.

Unfortunately, the relationship between α and β seems to be dependent on the particular dynamic excitation and, at this stage, an analytical expression has not been determined, still. Furthermore, it is worth to stress that small variations of the parameters α and β can produce some abrupt changes in the behaviour of the structure, in some cases amplifying the structural response. This is apparent in Figure 6, where the red area in the colour map is where the DSF panel actually worsen the seismic response of the primary frame. Hence, the relationship between

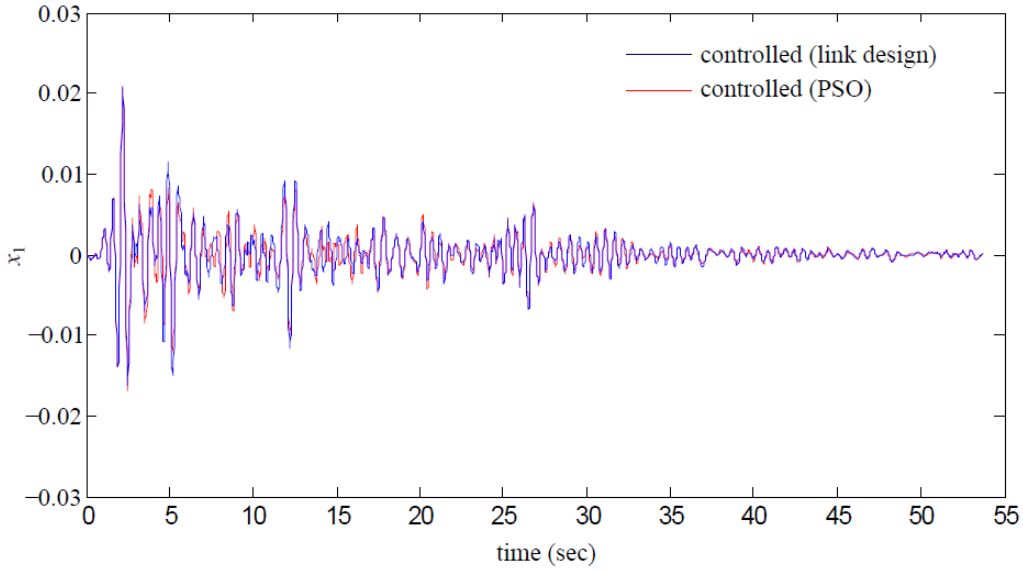

Figure 6: First storey displacements for El Centro 1940 earthquake: uncontrolled vs controlled system.

α and β should be assessed with the maximum possible accuracy, and a robust methodology needs to be devised.

4 Conclusions and future works

The paper has demonstrated that optimally tuned double-skin façades (DSFs) can be engineered as vibration absorbers to mitigate the effects of earthquake loadings on building structures. A very simple case study has been presented to prove the concepts, revealing that DSF panels can reduce the seismic response up to 35% of the uncontrolled case. Both GAs (Genetic Algorithms) and PSO (Particle Swarm Optimisation) have been used to find the optimal design parameters for the DSF panels, with the PSO showing in general a better performance. A closer look analysis of the optimal parameters for a set of twenty recorded accelerograms, with different characteristics in terms of duration and frequency content, has suggested a less cumbersome and more direct design strategy. That is, once the mass ratio between primary frame and the DSF has been fixed, along with its flexural stiffness and damping, the stiffness of the links to the primary frame can be chosen by considering a well-defined optimal region in the corresponding response surface. Interestingly, although similar performance can be achieved, very different dynamics of the DSF panels can be obtained by varying the stiffness of the links.

Encouraged by the positive results of this preliminary study, further research is planned. Future work will be devoted to the case of wind loadings and multi-hazard scenario (combined wind and earthquake cases). The effects of nonlinear behaviour and uncertainties in both the primary frame and in the DSF will be explored. Further

configurations of the outer panels will be considered as well, along with the case of taller buildings, in excess of twenty storeys.

Acknowledgments

The financial contribution of the Loughborough's Graduate School to AK's internship at Loughborough University is gratefully acknowledged.

References

[1] P. Abtahi, B. Samali, M. Zobec and T. Ngo, "Application of flexible façade systems in reducing the lateral displacement of concrete frames subjected to seismic loads", Proc. 22nd Australasian Conf. on the Mechanics of Structures and Materials, 241-245, 2013.

[2] A. K. Chopra, Dynamics of Structures, 4th Ed., Prentice-Hall, 2011.

[3] T. S. Fu, "Double skin façades as mass dampers", Proc. American Control Conf., 4742-4746, 2013.

[4] D. E. Goldberg, Genetic Algorithms in Search, Optimization & Machine Learning, Addison-Wesley, 1989.

[5] W.C. Hurty, "Vibrations of structural systems by component-mode synthesis", Journal of Engineering Mechanics Division, 86(4), 51–70, 1960.

[6] S. Kasinos, A. Palmeri and M. Lombardo, "Seismic response of combined primary-secondary structures with the component-mode synthesis method", Proc. 15th Int. Conf. on Civil, Structural and Environmental Engineering Computing, 2015 (accepted).

[7] J. E. Kennedy, R. C. Eberhart, "Particle Swarm Optimization", Proc. IEEE International Conference on Neural Networks, 1942-1948, 1995.

[8] K. S. Moon, "Tall building motion control using double skin façades", Journal of Architectural Engineering, 15(3), 84-90, 2009.

[9] K. S. Moon, "Structural design of double skin façades as damping devices for tall buildings", Procedia Engineering 14: 1351-1358, 2011.

[10] G. Muscolino, "Dynamic response of multiply connected primary-secondary systems", Earthquake Engineering & Structural Dynamics, 19(2), 205-216, 1990.

[11] G. Muscolino and A. Palmeri, "An earthquake response spectrum method for linear light secondary substructures", ISET Journal of Earthquake Technology, 44(1), 193-211, 2007.